JOURNAL OF SPACECRAFT AND ROCKETS
Vol. 35, No. 3, May–June 1998

Mars Free Return Trajectories

Moonish R. Patel*
Lockheed Martin Missiles and Space Company, Sunnyvale, California 94089
James M. Longuski†
Purdue University, West Lafayette, Indiana 47907-1282
and
Jon A. Sims‡
Jet Propulsion Laboratory, California Institute of Technology, Pasadena, California 91109-8099

For human missions to Mars, the top priority is a safe return of the crew to Earth. In the case of an emergency, trajectories that naturally return to the Earth with no intervention are preferred. We use automated design software to compute all possible Mars free return trajectories from 1995 to 2020, given constraints on the total time of flight and on the launch energy. The resulting data file contains all of the previously known types of returns. Because Earth and Mars return to the same inertial positions every 15 years, these results are representative of all Mars free returns. Of particular interest are two families of fast free returns (having times of flight of about 1.4 years) that occur in 2000 and 2002 and repeat in 2015 and 2017.

Nomenclature

a	= semimajor axis, AU
e	= eccentricity
j, k, m, n	= small positive integers
M_1	= primary body (sun)
M_2	= secondary body (Earth)
M_3	= spacecraft
V_∞	= hyperbolic excess velocity, km/s
ΔV	= change in velocity, km/s
η	= eccentric anomaly of M_3 during collision, rad
τ	= eccentric anomaly of M_2 during collision, rad

Introduction

THE anticipation of a human mission to Mars in the next millennium has stimulated a number of mission analysis studies. These studies include important topics such as propulsion options,[1,2] effect of delays,[3] abort options,[4] and trajectory options.[5] In most of these papers and in several others (for example, Refs. 6–8), the authors identify various classes of trajectories including opposition, sprint, conjunction, free return, and cycler. (An excellent survey of various mission scenarios is given by Walberg.[9]) Opposition class missions are characterized by a high-energy trajectory and a relatively short Mars stay time (less than 3 months). The name stems from the fact that the Earth leaves opposition with Mars at the Mars arrival. The total mission duration for this class ranges from 1 to 2.5 years. A subset of the opposition class is the sprint class. This class has a mission duration of approximately 1 to 1.4 years with a 30-day stay time. Sprint missions are intended for piloted missions because of their short flight times, but they have higher ΔV requirements. The most traditional mission class is the conjunction class. In this class the Earth is moving into conjunction with Mars at the time of Mars arrival. These missions are characterized by low-energy trajectories and have a relatively long stay time (0.8 to 1.5 years). They can be used during the early exploratory phase where many tasks need to be done on the planetary surface.

Received Aug. 5, 1997; revision received Jan. 30, 1998; accepted for publication Jan. 31, 1998.

*Senior Systems Engineer, Organization K2-46, Building 150, 1111 Lockheed Martin Way. Member AIAA.
†Associate Professor, School of Aeronautics and Astronautics. Associate Fellow AIAA.
‡Member of Engineering Staff, Navigation and Flight Mechanics Section, Mail Stop 301-142, 4800 Oak Grove Drive. Member AIAA.

For initial piloted missions, the free return class will most likely be the mission of choice because these trajectories do not require a deterministic maneuver to return the spacecraft to the Earth in the event of an emergency, e.g., Apollo 13. A subset of the free return class is the cycler class,[8] which includes VISIT (versatile international station for interplanetary transport) and up/down escalator (Aldrin) cyclers. Both of these cyclers repeatedly encounter the Earth and Mars. VISIT-I orbits have a 1.25-year period and encounter the Earth every 5 years and Mars every 3.75 years. VISIT-II orbits, on the other hand, have a period of 1.5 years and encounter the Earth once every 3 years and Mars every 7.5 years. The up/down escalator cycler (described in Ref. 10) is composed of multiple free return trajectories to Mars connected by Earth gravity assists. The Earth gravity assist rotates the major axis of the orbit so that the phasing will be correct for a Mars encounter on the next leg. The escalator orbits have an average Earth-to-Earth transfer time of 2.14 years, which is the Earth–Mars synodic period.

Advanced software developed by Patel[11] allows automated searches for multiple-encounter ΔV gravity-assist trajectories. This automated search algorithm (based on an earlier version developed by Williams[12]) solves the restricted n-body problem using the patched–conic theory described in Ref. 13. Reference 14 demonstrates that for interplanetary trajectories the patched–conic theory is reasonably accurate. References 15–22 demonstrate that this algorithm not only can identify known trajectories but also can be used to discover new trajectories much more efficiently.

In this paper we use the algorithm to compute all possible Mars free return trajectories with times of flight (TOFs) less than 4 years and for low-to-moderate launch energies. Our purpose is to present a compilation of all of the types of Mars free return trajectories and to show where these trajectories fit within the 15-year recurrence period.

Numerical Study

Considerable insight into the numerical results can be gained by recalling that the orbital period of Mars can be approximated (to three significant figures) by $1\frac{7}{8}$ years. This implies that the Earth–Mars synodic period is about $2\frac{1}{7}$ years. Thus in $2\frac{1}{7}$ years the two planets repeat their relative positions in space, but these positions advance by $\frac{1}{7}$ of a circle (51.4 deg) in inertial space. In seven synodic periods (about 15 years) the inertial positions repeat.

Figure 1 shows the result of the search for Mars free return trajectories for launch dates ranging from 1995 to 2020 with various launch V_∞ of 4, 5, 6, 7, and 8 km/s. (See Table 1 for legend for launch date plots.) Each number on the plot corresponds to a trajectory from Earth to Mars and back to Earth. We hasten to point out that, given the large number of trajectories, the individual numbers (0, 2, 3, 4,

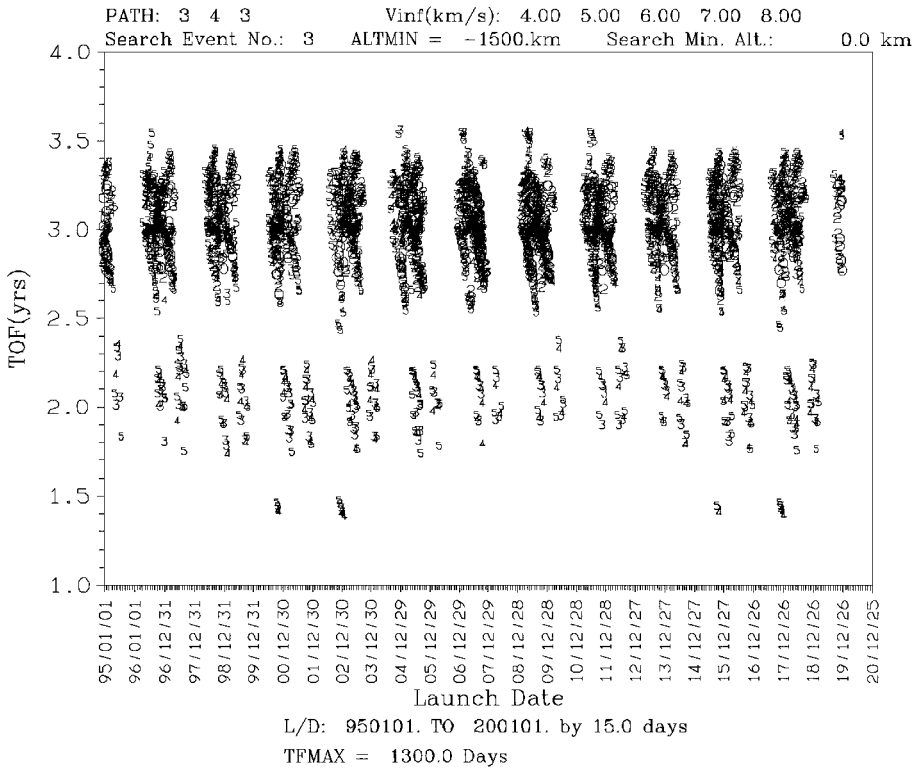

Fig. 1 Mars free return (1995–2020).

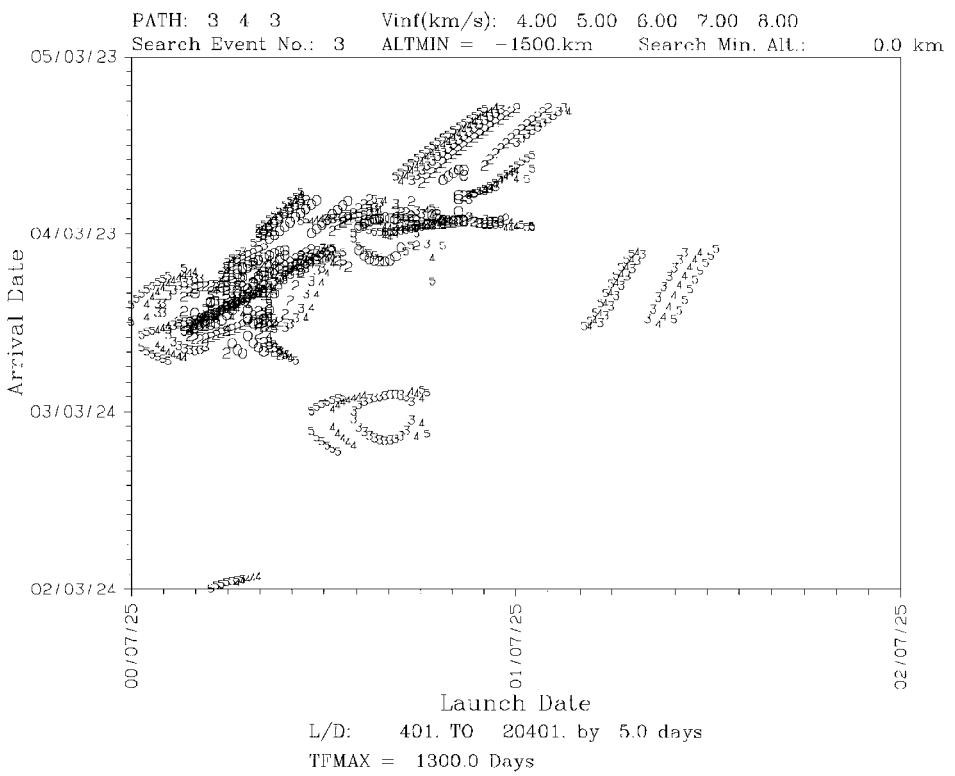

Fig. 2 Mars free return (2000–2002).

and 5) in Fig. 1 are difficult to discern. However, because our objective at this point is to observe the overall trends, the readability of the numbers is of little concern. Because the inertial positions of Earth and Mars repeat approximately every 15 years, the search over the 25-year span of launch dates represents all possible free return families (for 4 km/s $\preceq V_\infty \preceq$ 8 km/s). We note that the two sets of fast trajectories (TOF $\approx$ 1.4 years) during 2000 and 2002 repeat during 2015 and 2017 (15 years later). Figure 2 shows a close-up of the launch date/arrival date plot for launch dates in 2000–2002.

Many of these trajectories have high launch energy requirements and high Mars arrival V_∞. Among these are opposition class trajectories. Figure 3 shows a typical conic trajectory for this class. We see that the Mars gravity assist has a large effect on the trajectory; therefore, these orbits cannot be analyzed as small perturbations of collision orbits (which naturally reencounter the Earth with no gravity assist or deep-space maneuver). The analysis of collision orbits (which we discuss later) will improve the understanding of many of the families but cannot predict all of them precisely.

Table 1 Legend for launch date plots

PATH	Sequence of planets encountered. For example, PATH: 3 4 3 implies Earth–Mars–Earth in Fig. 1.
Vinf	Launch V_∞. The values of V_∞ in the plot itself are designated by 0, 2, 3, ... (0 was used in lieu of 1 because it is more easily distinguished). Thus the numeral 3 on the plot refers to a V_∞ of 6.0 km/s.
ALTMIN	Minimum flyby altitude allowed in the original run
L/D	Launch date range in calendar dates, where 950101 refers to Jan. 1, 1995. The launch date increment is also given for example, "BY 15 DAYS."
TFMAX	Maximum allowable time of flight
Search Event No.	Event in PATH sequence for which the plot is made. For example, Search Event No.: 3 implies that the TOF in Fig. 1 corresponds to the third event in the sequence, namely Earth (3) arrival.
Search Min. Alt.	Minimum flyby altitude allowed. For example, if the original file was created with ALTMIN = −1500 km, then Search Min. Alt. = 0.0 km would filter out the trajectories with flyby altitudes below 0.0 km.

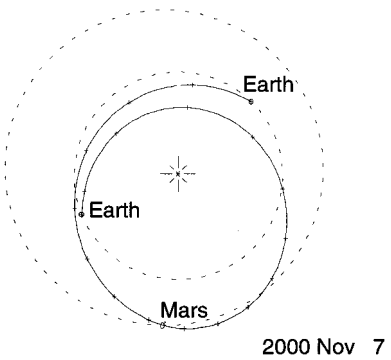

Fig. 3 Mars free return: opposition (TOF = 1.4 years).

We also note in Fig. 1 that the trajectories occur in three ranges of flight time around 1.5, 2, and 3 years. The spacing of about $2\frac{1}{7}$ years between launch windows is, of course, driven by the synodic period. In the case of TOF ≈ 2 years, the reason for a second set of windows, offset by about 0.6 years, is due to the fact that, for escalator orbits (which we will discuss later), there are two opportunities to encounter Mars in free return trajectories: one before aphelion of the trajectory and one after aphelion.

From an energy point of view, a Hohmann ellipse between the Earth and Mars would be the most desirable transfer because the launch and arrival V_∞ are minimized. For circular, coplanar orbits a minimum energy transfer between Earth and Mars has an orbital period of 1.42 years. It would therefore be impossible to return to the Earth in a single revolution after such a transfer because the Earth would not be in the correct position. Also because the orbital period does not form an integer ratio with the Earth's period, it would be impossible to return to the Earth within a few revolutions about the sun.

Wolf[23] shows that a free return trajectory with low launch energy and low arrival V_∞ can exist if the trajectories have orbital periods that are resonant with the Earth and Mars:

$$n\,(\text{orbital period}) = m\,(\text{Earth period})$$

$$j\,(\text{orbital period}) = k\,(\text{Mars period})$$

A subset of these trajectories is the VISIT cycler orbits. The VISIT-I orbit $[(n, m, j, k) = (4, 5, 3, 2)]$ is not included in the present analysis because of the long flight time between Earth encounters (5 years). Recall that the VISIT-II orbits $[(n, m, j, k) = (2, 3, 5, 4)]$ return to the Earth every 3 years and have a 1.5-year period. As Fig. 1 demonstrates, the majority of the Mars free return trajectories have flight times near 3 years.

For a transfer orbit with periapsis lower than Earth's orbit and apoapsis higher than Mars' orbit, there are many permutations of encounter positions for a given orbital period. Trajectories completing up to (about) one revolution can have the following encounter sequences (see Fig. 4): case 1, E1–M2–E1; case 2, E1–M2–E2; case 3, E1–M1–E1; case 4, E1–M1–E2; case 5, E2–M2–E1; case 6, E2–M2–E2; case 7, E2–M1–E1; and case 8, E2–M1–E2, where 1 refers to encounters (with Earth or Mars) before periapsis and 2 refers to encounters after periapsis. When up to (about) two complete revolutions are considered, there are twice as many permutations because M1 or M2 can occur on one of two revolutions. Figure 5 shows a conic trajectory representing case 8 with an orbital period of 1.5 years and a Mars encounter on the first revolution (type II) of a 3-year transfer.

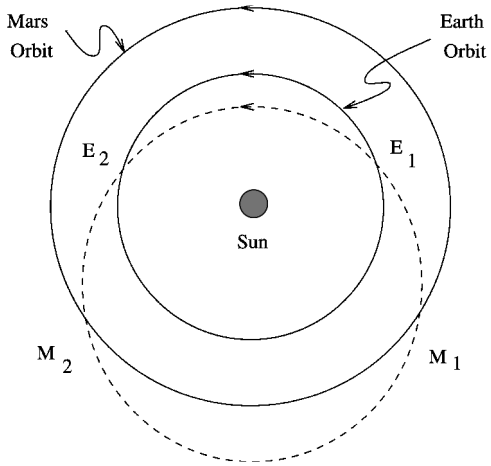

Fig. 4 Mars free return options.

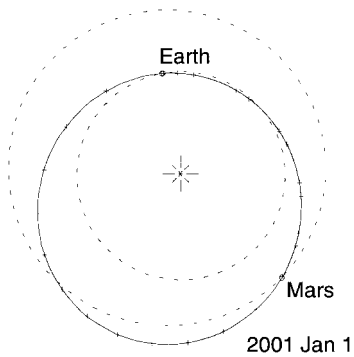

Fig. 5 Mars free return: 1.5-year period (TOF = 3.0 years) (E2–M1–E2).

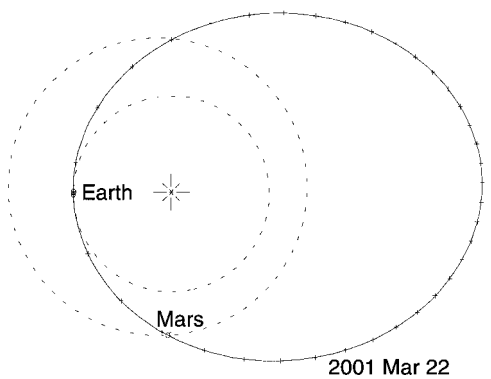

Fig. 6 Mars free return: 3.0-year period (TOF = 3.0 years).

Some of the free returns with a flight time of 3 years have an orbital period of 3 years. Because the spacecraft does not orbit the sun more than once, fewer such trajectories of this type exist when compared with the number of trajectories with an orbital period of 1.5 years. (See Fig. 6 for a conic trajectory example.)

A subset of the trajectories with a flight time of 2 years is the escalator orbit, which has an orbital period of about 2.02 years and an Earth V_∞ of about 6.0 km/s. Examples of both up and down escalators are shown in Table 2. Here we see that the TOF between

Table 2 Up/down-escalator orbits (from Ref. 10)

	Up escalator		Down escalator	
Encounter	Date	Approach V_∞ or ΔV, km/s	Date	Approach V_∞ or ΔV, km/s
Earth-1	Nov. 19, 1996	6.19	June 5, 1995	5.88
Mars-2	May 1, 1997	10.69	Jan. 20, 1997	8.52
Earth-3	Jan. 1, 1999	5.94	July 9, 1997	5.95
Mars-4	May 28, 1999	11.74	March 7, 1999	7.35
Earth-5	Feb. 8, 2001	5.67	Aug. 17, 1999	6.01
Maneuver	——	——	Sept. 28, 2000	0.27
Mars-6	July 6, 2001	10.22	May 15, 2001	6.60
Maneuver	March 13, 2002	0.54	——	——
Earth-7	April 16, 2003	5.67	Oct. 8, 2001	5.88
Maneuver	——	——	Dec. 4, 2002	1.11
Mars-8	Sept. 12, 2003	7.28	Aug. 7, 2003	7.30
Maneuver	May 17, 2004	0.74	——	——
Earth-9	July 7, 2005	5.87	Jan. 2, 2004	5.39
Maneuver	——	——	Feb. 2, 2005	0.66
Mars-10	Dec. 13, 2005	6.05	Oct. 10, 2005	9.96
Maneuver	July 23, 2006	0.45	——	——
Earth-11	Sept. 6, 2007	5.87	March 12, 2006	5.48
Mars-12	Feb. 16, 2008	7.43	Nov. 19, 2007	11.59
Earth-13	Oct. 10, 2009	5.89	April 16, 2008	5.96
Mars-14	March 28, 2010	8.66	Dec. 13, 2009	10.55
Earth-15	Nov. 13, 2011	5.81	May 22, 2010	5.93

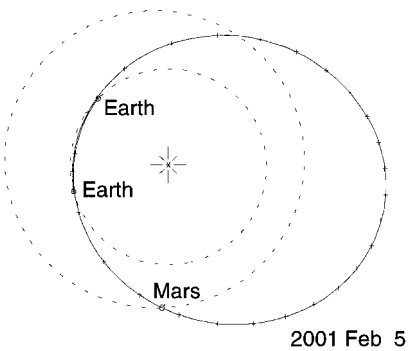

Fig. 7 Mars free return: up escalator.

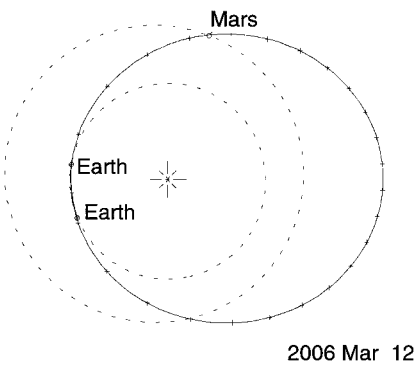

Fig. 8 Mars free return: down escalator.

Earth-1 and Earth-3 for the up escalator is about 2.12 years (very close to the synodic period of 2.14 years). We can also see that the calendar difference between Earth-1 of the up escalator and Earth-3 of the down escalator is about 7 months and 20 days, or 0.63 years. This difference is consistent with the 0.6-year gaps observed in Fig. 1. In Fig. 2 variations of the up-escalator family are indicated by the first set of closed contours (of threes) for launch dates in the month of March 2001 with arrival dates in March 2003. Variations of the down-escalator family are shown by the contours near the launch date in October 2001. The escalator orbits are entirely contained within the launch date/arrival date data, i.e., trajectories in Table 2 are all included in Fig. 1. Maneuvers are sometimes required to maintain the cyclers because the Earth may not provide sufficient bending to rotate the line of apsides. Figures 7 and 8 show examples of up- and down-escalator trajectories.

Consecutive Collision Orbits

Free return trajectories with a small body such as Mars are very similar to collision orbits. A collision orbit is an orbit that encounters an object, e.g., Earth, twice within a certain time. By assuming that a flyby of a second small body, e.g., Mars, only slightly perturbs the orbit, this type of orbit can easily be used to analyze the Mars free return problem. An analytical approach to solving the consecutive collision problem is described by Hénon.[24] This work not only addresses the problem of the simple case where the two encounters occur at the same point in space but also solves the more complicated problem in which the two encounters take place at different points in space. Howell[25] extends this solution to solve for consecutive collision orbits in the elliptic restricted problem. Prado and Broucke[26] show how to solve Hénon's orbit transfer problem for any type of orbit (elliptic, parabolic, or hyperbolic) by using the Lambert algorithm. Because the eccentricity of the Earth's orbit is quite small, Hénon's circular approximation is sufficient for this very preliminary comparison of theoretical predictions and numerical results.

A brief summary of the results obtained by Hénon is as follows. Unit length and time are selected based on the secondary body M_2 (the Earth). Now, from Fig. 9, the collision points are denoted P and Q and the time interval between the collisions is 2τ. Taking the middle of the interval as time $t = 0$, the collisions between the Earth and the spacecraft (M_3) occur at $-\tau$ and τ. Different orbit types are described by the following parameters:

$$\varepsilon = \begin{cases} +1 \\ -1 \end{cases} \quad \text{if } M_3 \text{ periapsis} \begin{cases} \text{positive} \\ \text{negative} \end{cases}$$

$$\varepsilon' = \begin{cases} +1 \\ -1 \end{cases} \quad \text{if } M_3 \text{ orbit} \begin{cases} \text{direct} \\ \text{retrograde} \end{cases}$$

$$\varepsilon'' = \begin{cases} +1 \\ -1 \end{cases} \quad \text{if } M_3 \text{ at } t = 0 \begin{cases} \text{periapsis} \\ \text{apoapsis} \end{cases}$$

At the time of collision, the eccentric anomalies of M_2 and M_3 are τ and η, respectively. For elliptical transfers, the solution for the transfer orbit can be obtained by solving the following implicit timing equation relating τ and η:

$$\sqrt{1 - \varepsilon\varepsilon'' \cos\tau \cos\eta}\,[\eta(1 - \varepsilon\varepsilon'' \cos\tau \cos\eta) - \sin\eta(\cos\eta - \varepsilon\varepsilon'' \cos\tau)] - \tau|\sin\eta|^3 = 0 \tag{1}$$

Table 3 Excerpt from Hénon's tables[24]

τ/π, yr	η/π	Semimajor axis, AU	Eccentricity	Period, yr
2.00000	1.00000	1.58740	0.37004	2.00141
3.00000	2.00000	1.31037	0.23686	1.50003
3.00000	1.00000	2.08008	0.51925	3.00083

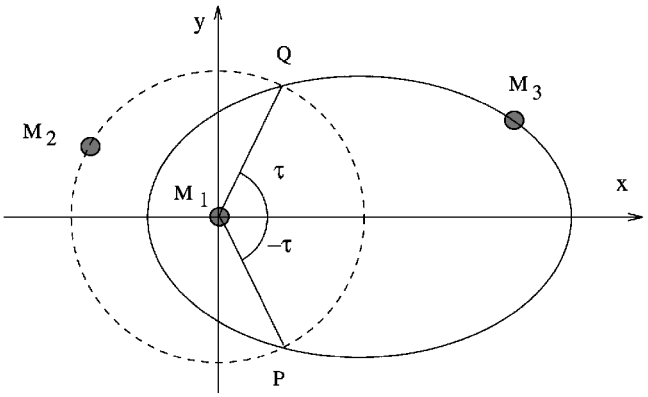

Fig. 9 Collision orbits.

Once τ and η are known, the transfer orbit can be determined from

$$a = \frac{1 - \varepsilon\varepsilon'' \cos\tau \cos\eta}{\sin^2\eta} \tag{2}$$

$$e = \frac{\varepsilon'' \cos\eta - \varepsilon \cos\tau}{1 - \varepsilon\varepsilon'' \cos\tau \cos\eta} \tag{3}$$

Hénon presents numerous tables containing solutions of Eq. (1), that is, various combinations of τ and η that solve the timing condition. We use these tables in our analysis. They include the values for η/π (number of revolutions), τ/π (flight time in Earth years), orbit type, a, and e; thus, they represent numerous trajectories that depart from Earth and reencounter the Earth after a specified time interval.

The Hénon consecutive collision orbits can be used to predict free return trajectories to Mars by the addition of a constraint: The aphelion of the collision orbit must be greater than the orbital radius of Mars. Several trajectories obtained from numerical analysis appear in Hénon's tables[24]; a few of these trajectories are summarized in Table 3. Further research in this area might be fruitful in analytically predicting free return trajectories. The orbits that have large Mars flyby altitudes are in fact the collision orbits predicted by Hénon.[24] It is important to note, however, that the gravity of Mars can cause large perturbations to the trajectories as demonstrated with the fast TOF trajectories (e.g., see Fig. 3), and thus the analysis might be more useful if generalized to include this effect.

Conclusion

Recently developed automated design software for the analysis of gravity-assist trajectories has permitted a thorough investigation of Mars free return trajectories. The resulting data file contains a variety of well-known trajectory classes. The analysis of Hénon helps verify some of these numerical results.

Low-energy free returns with TOFs around 3 years (or less) are plentiful and occur every synodic period. Higher-energy free returns with TOFs around 2 years are also plentiful and occur synodically. Of particular interest are fast free returns that occur in 2015 and 2017 and have the shortest TOF of about 1.4 years. These trajectories may provide a timely opportunity for the first human mission to Mars.

Acknowledgment

Portions of the work described were performed at the Jet Propulsion Laboratory, California Institute of Technology, under contract with NASA.

References

[1]Braun, R. D., and Blersch, D. J., "Propulsive Options for a Manned Mars Transportation System," *Journal of Spacecraft and Rockets*, Vol. 28, No. 1, 1991, pp. 85–92.

[2]Striepe, S. A., and Desai, P. N., "Piloted Mars Missions Using Cryogenic and Storable Propellants," *Journal of the Astronautical Sciences*, Vol. 44, No. 2, 1996, pp. 207–222.

[3]Desai, P. N., and Tartabini, P. V., "Effect of Departure Delays on Manned Mars Mission Selection," *Journal of Spacecraft and Rockets*, Vol. 32, No. 2, 1995, pp. 250–256.

[4]Tartabini, P. V., Striepe, S. A., and Powell, R. W., "Abort Options for Potential Mars Missions," *Journal of Spacecraft and Rockets*, Vol. 31, No. 4, 1994, pp. 543–549.

[5]Braun, R. D., "The Influence of Interplanetary Trajectory Options on a Chemically Propelled Manned Mars Mission," *Journal of the Astronautical Sciences*, Vol. 38, No. 3, 1990, pp. 289–310.

[6]Hoffman, S. J., McAdams, J. V., and Niehoff, J. C., "Round Trip Trajectory Options for Human Exploration of Mars," American Astronautical Society, AAS 89-201, Greenbelt, MD, April 1989.

[7]Niehoff, J. C., "Pathways to Mars: New Trajectory Opportunities," American Astronautical Society, AAS 86-172, Washington, DC, July 1986.

[8]Friedlander, A., Niehoff, J., Byrnes, D., and Longuski, J., "Circulating Transportation Orbits Between Earth and Mars," AIAA Paper 86-2009, Aug. 1986.

[9]Walberg, G., "How Shall We Go To Mars? A Review of Mission Scenarios," *Journal of Spacecraft and Rockets*, Vol. 30, No. 2, 1993, pp. 129–139.

[10]Byrnes, D. V., Longuski, J. M., and Aldrin, B., "The Cycler Orbits Between Earth and Mars," *Journal of Spacecraft and Rockets*, Vol. 30, No. 3, 1993, pp. 334–336.

[11]Patel, M. R., "Automated Design of Delta–V Gravity Assist Trajectories for Solar System Exploration," M.S. Thesis, School of Aeronautics and Astronautics, Purdue Univ., West Lafayette, IN, Aug. 1993.

[12]Williams, S. N., "Automated Design of Multiple Encounter Gravity-Assist Trajectories," M.S. Thesis, School of Aeronautics and Astronautics, Purdue Univ., West Lafayette, IN, Aug. 1990.

[13]Battin, R. H., *An Introduction to the Mathematics and Methods of Astrodynamics*, AIAA Education Series, AIAA, New York, 1987, pp. 419–470.

[14]Breakwell, J. V., and Perko, L. M., "Matched Asymptotic Expansions, Patched Conics and the Computation of Interplanetary Trajectories," AIAA Paper 65-689, Sept. 1965.

[15]Longuski, J. M., and Williams, S. N., "The Last Grand Tour Opportunity to Pluto," *Journal of the Astronautical Sciences*, Vol. 39, No. 3, 1991, pp. 359–365.

[16]Williams, S. N., and Longuski, J. M., "Automated Design of Multiple Encounter Gravity-Assist Trajectories," AIAA Paper 90-2982, Aug. 1990.

[17]Longuski, J. M., and Williams, S. N., "Automated Design of Gravity-Assist Trajectories to Mars and the Outer Planets," *Celestial Mechanics and Dynamical Astronomy*, Vol. 52, No. 3, 1991, pp. 207–220.

[18]Williams, S. N., and Longuski, J. M., "Low Energy Trajectories to Mars via Gravity Assist from Venus and Earth," *Journal of Spacecraft and Rockets*, Vol. 28, No. 4, 1991, pp. 486–488.

[19]Patel, M. R., and Longuski, J. M., "Automated Design of Delta–*V* Gravity-Assist Trajectories for Solar System Exploration," American Astronautical Society, AAS Paper 93-682, Victoria, BC, Canada, Aug. 1993.

[20]Patel, M. R., Longuski, J. M., and Sims, J. A., "A Uranus-Neptune-Pluto Opportunity," *Acta Astronautica*, Vol. 36, No. 2, 1995, pp. 91–98.

[21]Sims, J. A., Staugler, A. J., and Longuski, J. M., "Trajectory Options to Pluto via Gravity Assists from Venus, Mars, and Jupiter," *Journal of Spacecraft and Rockets*, Vol. 34, No. 3, 1997, pp. 347–353.

[22]Sims, J. A., Longuski, J. M., and Staugler, A. J., "Trajectory Options for Low-Cost Missions to Asteroids," Second IAA International Conf. on Low-Cost Planetary Missions, IAA-L-0206, Laurel, MD, April 1996; also *Acta Astronautica* (to be published).

[23]Wolf, A. A., "Free Return Trajectories for Mars Missions," American Astronautical Society, AAS Paper 91-123, Houston, TX, Feb. 1991.

[24]Hénon, M., "Sur les Orbites Interplanétaires qui Recontrent Deux Fois la Terre," *Bulletin Astronomique*, Vol. 3, 1968, pp. 377–402.

[25]Howell, K. C., "Consecutive Collision Orbits in the Limiting Case $\mu = 0$ of the Elliptic Restricted Problem," *Celestial Mechanics*, Vol. 40, 1987, pp. 393–407.

[26]Prado, A. F. B. A., and Broucke, R. A., "Study of Hénon's Orbit Transfer Problem Using the Lambert Algorithm," *Journal of Guidance, Control, and Dynamics*, Vol. 17, No. 5, 1994, pp. 1075–1081.

J. A. Martin
Associate Editor